PROGRESS IN AEROSPACE AND AVIATION TECHNOLOGY
e-ISSN: 2821-2924

PAAT

Vol. 4 No. 2 (2024) 76-87
https://publisher.uthm.edu.my/ojs/index.php/paat

Investigating Aerodynamic Characteristics of a Fixed-Wing Hybrid UAV During Hover-Forward Transition Flight Phase

Muhammad Munib Abid Aqeel[1], Mohd Fadhli Zulkafli[2]*, Mohammad Fahmi Pairan[2]

[1] *Department of Mechanical Engineering, Faculty of Mechanical and Manufacturing Engineering, Universiti Tun Hussein Onn Malaysia, 86400 Batu Pahat, Johor, MALAYSIA*

[2] *Research Centre for Unmanned Vehicle, Faculty of Mechanical and Manufacturing Engineering, Universiti Tun Hussein Onn Malaysia, 86400 Batu Pahat, Johor, MALAYSIA*

*Corresponding Author: fadhli@uthm.edu.my

DOI: https://doi.org/10.30880/paat.2024.04.02.008

Article Info

Received: 29 June 2024
Accepted: 10 November 2024
Available online: 24 December 2024

Keywords

UAV, fixed wing, VTOL, hybrid UAV, simulation, tricopter

Abstract

In the past few years, unmanned aerial vehicles (UAVs) have been employed extensively in agricultural observation, wildlife protection, and traffic monitoring sectors. Hybrid UAVs combine the advantages of both multirotor and fixed-wing types, which can take off and land vertically. The key objective of the present work is to investigate the aerodynamic characteristics of a vertical takeoff and landing (VTOL) fixed-wing Tricopter (VFW tricopter) UAV by creating a 3D model in Plane-Maker and simulating that model to get thrust, lift force, drag force, and static pitch stability. X-Plane 12 was used to design and study the aerodynamic characteristics of a VTOL Tricopter UAV during the hover-forward transition flight phase. It has been found that the value of thrust force was high before transition, which is suitable for vertical takeoff and maneuvering. During the transition, it starts decreasing. After the transition, the thrust goes down and then stabilizes at lower values to sustain forward motion. This thrust reduction enables the plane to glide. In terms of pitch stability, at the beginning of the transition phase, the VFW tricopter UAV was unstable. Afterwards, the pitch stability stabilizes, indicating that the UAV has adjusted to a stable forward flight. Transition thrust vector changes may cause instability at the start of the transition phase. Lift force was high and stable during hover, decreased during transition, and showed fluctuations as the tricopter UAV adjusted to forward flight. Drag force was relatively high during hover and decreased during transition, stabilizing at lower values during forward flight. The frontal area of the tricopter UAV decreased, which caused the plane to produce less drag. This study aids in designing and understanding the aerodynamic characteristics of a VFW tricopter UAV during the hover-forward transition flight phase.

1. Introduction

In recent years, civil unmanned aerial vehicles (UAVs) have been used widely in areas such as agricultural observation, wildlife protection, and traffic monitoring. There are various types of UAVs, such as multirotor and fixed-wing (FW) UAVs. Multirotor UAVs, which consist of multiple rotors, possess certain advantages when compared to traditional unmanned aerial platforms such as airplanes and helicopters. Fixed-wing unmanned aerial vehicles (UAVs) consist of a fuselage, wings, and tail, with a motor and propeller acting as the primary propulsion system platform [1]. They possess greater top speeds than multirotor UAVs, rendering them more appropriate for applications like aerial mapping, monitoring, and surveillance. Different operational aims shape the design of each type of UAV [2].

Fixed-wing hybrid UAVs offer the benefits of both multirotor and fixed-wing types. They can take off and land vertically (VTOL) like multirotors and travel long distances like fixed-wing UAVs. Depending on their propulsion type, hybrid UAVs can be further divided into two categories: those with the same propulsion for vertical and horizontal flight and those with separate propulsion for each flight mode. The former includes tilt-wing, tiltrotor, and tail sitter UAVs, while the latter includes VTOL fixed wing (VFW). The VFW UAV is simple to implement and can be further expanded with quadrotors and fixed-wing configuration [3], [4].

The VTOL fixed wing tricopter (VFW tricopter) UAV consists of 3 rotors, two at the front and one at the tail of the plane. VFW tricopter UAVs use tiltrotors for vertical takeoff and landing. The transition of VFM tricopter UAVs consists of four phases: take-off, transition, cruise, and landing. Firstly, the UAV takes off vertically using vector thrust. After hovering briefly, it transitions to forward flight. The transition process ends when the UAV reaches cruising altitude. However, the cruising range will be reduced due to the substantial amount of power required for vertical takeoff in order to attain cruising altitude [5]. In that order, the phases of flight with the highest power consumption are take-off, landing, and cruise. An excessive amount of energy is expended during a vertical takeoff since all three rotors are in motion.

Moreover, the development of a flight simulation structure for UAVs using the same techniques and subsystems enables the validation and verification of concepts and systems, optimization of the design, and additionally, the enhancement of flying techniques and performance [6]. The X-Plane flight simulator has remarkable precision in forecasting the aerodynamic behavior of the aircraft [7]. The X-Plane flight simulator operates on the principle of the blade element theory. X-Plane divides the aircraft into many small elements, and calculates the forces acting on each element several times per second. X-Plane provides realistic simulation. Laminar Research claims that using the blade element theory to calculate the forces on the aircraft is more accurate than the stability derivative method.

The design of a VFW UAV is the crucial step in building a UAV for better performance. The transition phase of vertical takeoff to horizontal flight of UAVs is also a critical point that determines the possibility and operational success of these systems. During this phase, the VFW UAV must shift from a hovering mode, relying on vertical thrust, to forward flight, which requires aerodynamic lift. This shift creates a complex control challenge, which is one of the reasons for accidents. Many studies discussed other types of VFW UAVs, but there is not enough knowledge regarding VFW tricopter UAVs. There is a lack of a comprehensive understanding of the specific aerodynamic characteristics which drive the VFW tricopter UAVs during transition flight. This knowledge gap is limiting the optimal utilization of these advanced aircraft, impacting their stability and performance. To solve this issue, this project aims to investigate the aerodynamic characteristics of VFW tricopter UAVs during the transition phase and provide valuable insights to unlock the full potential of hybrid UAVs. The study investigates the behavior of a VFW tricopter UAV during the hover-forward transition phase using computer simulation. The focus of this simulation model lies on important performance parameters like the thrust, stability, lift, and drag forces acting on the UAV during the flight phase.

2. Methodology

2.1 Plane-Maker (X-Plane)

This study uses the Plane-Maker software, which is an X-Plane program, to design the VFW tricopter model, as shown in Fig. 1. Similarly, Fig. 2 displays the model in wireframe view, along with the location of the CG. Plane-maker allows the user to create any type of aerial vehicle [8]. The program offers a visual interface for creating an airplane based on certain physical attributes, such as weight, engine power, wingspan, wing area, control surfaces, and the center of gravity [9]. X-Plane has the ability to forecast the flight characteristics of the aircraft [9]. The model details are in Table 1.

Fig. 1 *VFW tricopter UAV model in Plane-maker*

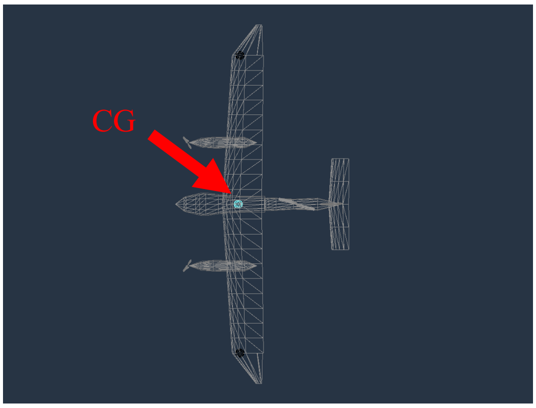

Fig. 2 *Wireframe view*

Table 1 *Design parameters*

Parameters	Values
Weight	Approx. 8.1 lb
Wingspan	1.5 meters
3 Motors (engine)	620 kV (each)
Centre of gravity (CG)	At 25% of the chord
Battery	6,000 mAh
Airfoil shape for the Wings	NACA 2412
Airfoil shape for Props	Clark Y
Propeller	3.6 inches

Measurements of the UAV's weight and specifications are necessary to create an accurate X-Plane flying model, as indicated in Table 1. The VFW tricopter UAV model consists of three motors, two at the front and one at the tail of the UAV. All three motors are modeled with a 3.6-inch propeller. After creating the design, the first step is to define the moving components of the UAV, such as the rudder, elevator, and ailerons. Then the engine parameters such as propeller RPM (revolutions per minute), size, and the location of motors (engines) need to be specified. The propeller and motor specifications window are shown in Fig. 3 and 4. To add VTOL capability to the fixed-wing UAV, the front two motors must move from 0 to 90 degrees at a tilt rate of 15 degrees per second, as demonstrated in Fig. 6. The value of the motor's input, such as "+1" provides the power to the aircraft, and the motor turns off when given "0". The weight and center of gravity play the most important role in the stability of the plane. The last step is to assign the weight and center of gravity, as shown in Fig. 5. The design that is created through the Plane-Maker software will be simulated using the X-Plane software, as explained in the following section.

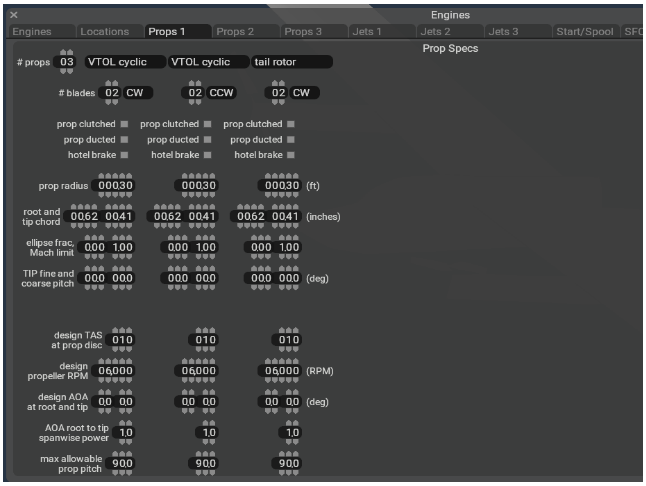

# props	03	VTOL cyclic	VTOL cyclic	tail rotor
# blades		02 CW	02 CCW	02 CW
prop clutched		■	■	■
prop ducted		■	■	■
hotel brake		■	■	■
prop radius		000.30	000.30	000.30 (ft)
root and tip chord		00.62 00.41	00.62 00.41	00.62 00.41 (inches)
ellipse frac, Mach limit		0.00 1.00	0.00 1.00	0.00 1.00
TIP fine and coarse pitch		00.0 00.0	00.0 00.0	00.0 00.0 (deg)
design TAS at prop disc		010	010	010
design propeller RPM		06,000	06,000	06,000 (RPM)
design AOA at root and tip		0.0 0.0	0.0 0.0	0.0 0.0 (deg)
AOA root to tip spanwise power		1.0	1.0	1.0
max allowable prop pitch		90.0	90.0	90.0

Fig. 3 *Input window for Propeller specification*

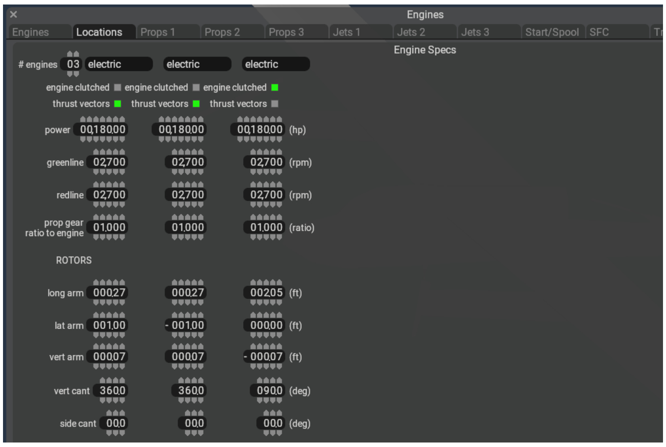

# engines	03 electric	electric	electric	
	engine clutched ☐	engine clutched ☐	engine clutched ☑	
	thrust vectors ☑	thrust vectors ☑	thrust vectors ☐	
power	00,180.00	00,180.00	00,180.00	(hp)
greenline	02,700	02,700	02,700	(rpm)
redline	02,700	02,700	02,700	(rpm)
prop gear ratio to engine	01.000	01.000	01.000	(ratio)
ROTORS				
long arm	000.27	000.27	002.05	(ft)
lat arm	001.00	- 001.00	000.00	(ft)
vert arm	000.07	000.07	- 000.07	(ft)
vert cant	360.0	360.0	090.0	(deg)
side cant	00.0	00.0	00.0	(deg)

Fig. 4 *Input window for Engine specification*

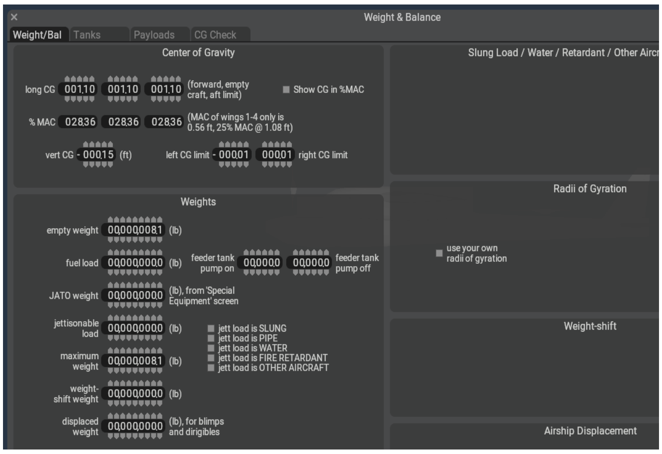

long CG 001.10 001.10 001.10 (forward, empty craft, aft limit) ☐ Show CG in %MAC
% MAC 028.36 028.36 028.36 (MAC of wings 1-4 only is 0.56 ft, 25% MAC @ 1.08 ft)
vert CG - 000.15 (ft) left CG limit - 000.01 000.01 right CG limit

empty weight 00,000,008.1 (lb)
fuel load 00,000,000.0 (lb) feeder tank pump on 00,000.0 00,000.0 feeder tank pump off
JATO weight 00,000,000.0 (lb), from 'Special Equipment' screen
jettisonable load 00,000,000.0 (lb)
☐ jett load is SLUNG
☐ jett load is PIPE
☐ jett load is WATER
☐ jett load is FIRE RETARDANT
☐ jett load is OTHER AIRCRAFT
maximum weight 00,000,008.1 (lb)
weight-shift weight 00,000,000.0 (lb)
displaced weight 00,000,000.0 (lb), for blimps and dirigibles
☐ use your own radii of gyration

Fig. 5 *Input window for Weight & center of gravity*

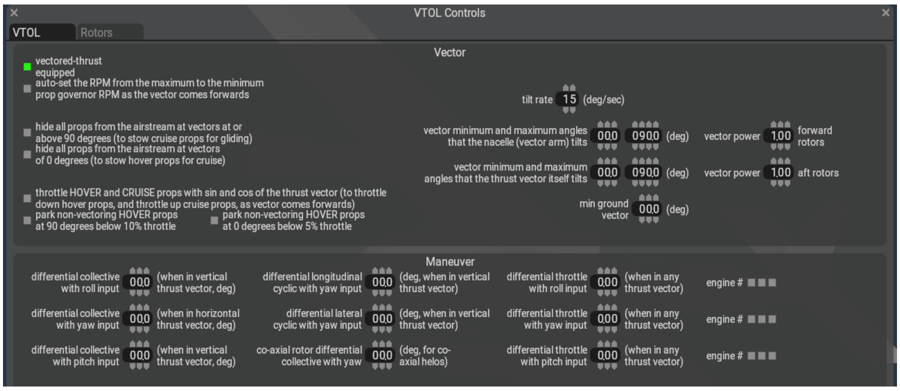

☑ vectored-thrust equipped
☐ auto-set the RPM from the maximum to the minimum prop governor RPM as the vector comes forwards
☐ hide all props from the airstream at vectors at or above 90 degrees (to stow cruise props for gliding)
☐ hide all props from the airstream at vectors of 0 degrees (to stow hover props for cruise)
☐ throttle HOVER and CRUISE props with sin and cos of the thrust vector (to throttle down hover props, and throttle up cruise props, as vector comes forwards)
☐ park non-vectoring HOVER props at 90 degrees below 10% throttle
☐ park non-vectoring HOVER props at 0 degrees below 5% throttle

tilt rate 15 (deg/sec)
vector minimum and maximum angles that the nacelle (vector arm) tilts 00.0 090.0 (deg) vector power 1.00 forward rotors
vector minimum and maximum angles that the thrust vector itself tilts 00.0 090.0 (deg) vector power 1.00 aft rotors
min ground vector 00.0 (deg)

differential collective with roll input 00.0 (when in vertical thrust vector, deg)
differential collective with yaw input 00.0 (when in horizontal thrust vector, deg)
differential collective with pitch input 00.0 (when in vertical thrust vector, deg)
differential longitudinal cyclic with yaw input 00.0 (deg, when in vertical thrust vector)
differential lateral cyclic with yaw input 00.0 (deg, when in vertical thrust vector)
co-axial rotor differential collective with yaw 00.0 (deg, for co-axial helos)
differential throttle with roll input 0.00 (when in any thrust vector) engine # ☐ ☐ ☐
differential throttle with yaw input 0.00 (when in any thrust vector) engine # ☐ ☐ ☐
differential throttle with pitch input 0.00 (when in any thrust vector) engine # ☐ ☐ ☐

Fig. 6 *Input window for VTOL requirement*

2.2 Simulation in X-Plane software

The flight simulator X-Plane was chosen because of its ability to predict the aircraft's flying qualities with high accuracy. This is performed by using the blade element theory. The software employs the blade element theory to generate the forces and moments acting on individual aircraft surfaces, and subsequently applies these processed results to the entire aircraft [7]. The software divides the aircraft into numerous small elements, calculating the forces acting on each element several times per second. X-Plane is a more advanced and adaptable flight simulator than competitors such as Flight Gear and FSX. Furthermore, X-Plane's simulation results are more reliable, earning it the distinction of being the only FAA-certified flight simulator [10]. Laminar Research claims that using the blade element theory to calculate the forces on the aircraft is more accurate than the stability derivative method. The X-Plane can simulate the cloud cover, rain, wind, thermals, microburst, and fog. This work utilizes X-Plane 12 to generate the tricopter model and simulate its dynamics, as illustrated in Fig. 7. The X-Plane is capable of producing a substantial amount of data. Fig. 8 displays the list of data outputs. The X-Plane provides the output data in the form of a text file where a user can check all flight data.

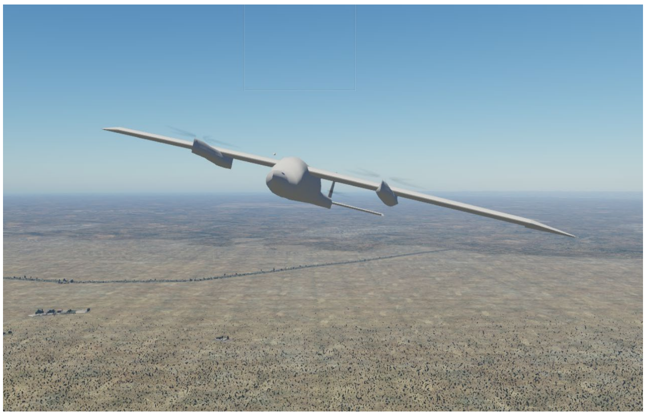

Fig. 7 *Hybrid tricopter UAV during flight in X-Plane*

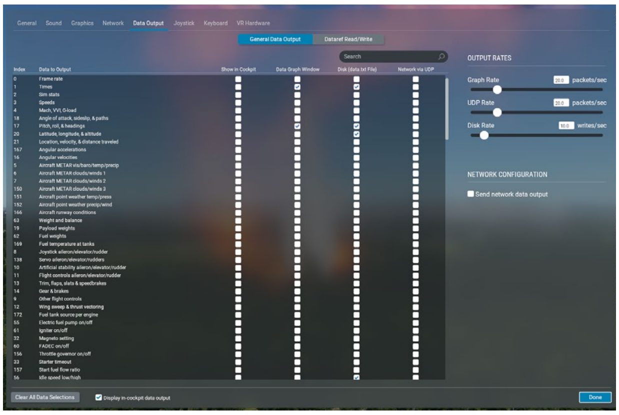

Index	Data to Output	Show in Cockpit	Data Graph Window	Disk (data.txt File)	Network via UDP
0	Frame rate	☐	☐	☐	☐
1	Times	☐	☑	☑	☐
2	Sim stats	☐	☐	☐	☐
3	Speeds	☐	☐	☐	☐
4	Mach, VVI, G-load	☐	☐	☐	☐
18	Angle of attack, sideslip, & paths	☐	☐	☐	☐
17	Pitch, roll, & headings	☐	☑	☑	☐
20	Latitude, longitude, & altitude	☐	☐	☑	☐
21	Location, velocity, & distance traveled	☐	☐	☐	☐
167	Angular accelerations	☐	☐	☐	☐
16	Angular velocities	☐	☐	☐	☐
5	Aircraft METAR vis/baro/temp/precip	☐	☐	☐	☐
6	Aircraft METAR clouds/winds 1	☐	☐	☐	☐
7	Aircraft METAR clouds/winds 2	☐	☐	☐	☐
150	Aircraft METAR clouds/winds 3	☐	☐	☐	☐
151	Aircraft point weather temp/press	☐	☐	☐	☐
152	Aircraft point weather precip/wind	☐	☐	☐	☐
166	Aircraft runway conditions	☐	☐	☐	☐
63	Weight and balance	☐	☐	☐	☐
19	Payload weights	☐	☐	☐	☐
62	Fuel weights	☐	☐	☐	☐
169	Fuel temperature at tanks	☐	☐	☐	☐
8	Joystick aileron/elevator/rudder	☐	☐	☐	☐
138	Servo aileron/elevator/rudders	☐	☐	☐	☐
10	Artificial stability aileron/elevator/rudder	☐	☐	☐	☐
11	Flight controls aileron/elevator/rudder	☐	☐	☐	☐
13	Trim, flaps, slats & speedbrakes	☐	☐	☐	☐
14	Gear & brakes	☐	☐	☐	☐
9	Other flight controls	☐	☐	☐	☐
12	Wing sweep & thrust vectoring	☐	☐	☐	☐
172	Fuel tank source per engine	☐	☐	☐	☐
55	Electric fuel pump on/off	☐	☐	☐	☐
61	Igniter on/off	☐	☐	☐	☐
32	Magneto setting	☐	☐	☐	☐
60	FADEC on/off	☐	☐	☐	☐
156	Throttle governor on/off	☐	☐	☐	☐
33	Starter timeout	☐	☐	☐	☐
157	Start fuel flow ratio	☐	☐	☐	☐
56	Idle speed low/high	☐	☐	☑	☐

☑ Display in-cockpit data output

OUTPUT RATES

Graph Rate 20.0 packets/sec

UDP Rate 20.0 packets/sec

Disk Rate 10.0 writes/sec

NETWORK CONFIGURATION

☐ Send network data output

Fig. 8 *Data output list window*

This study shows a way to use flight-time simulation to make correct-by-construction plans even better at being optimal. It is not novel to use simulations and optimizations to determine the best course of action during a UAV mission [11]. The parameters to be studied in this research are static pitch stability, thrust, lift, and drag of the VFW tricopter UAV over time during the hover-to-forward transition phase.

2.3 VTOL tricopter Design

This section involved creating a VTOL tricopter design using Plane-Maker and performing detailed simulations in X-Plane to analyze its static pitch stability, thrust, lift, and drag over time. Plane-Maker, the X-Plane program, facilitates the design process using the design parameters listed in Table 1. Fig. 9(a) and (d) show the isometric and top view of the tricopter VTOL plane. The design of the VTOL tricopter plane was a crucial aspect of this project. The plane model consists of three motors, two at the front and one at the tail of the aircraft. All three motors are modeled with a 3.6-inch propeller. The vector rotors in the front two motors can move from 0 to 90 degrees during transition, with a tilt rate of 15 degrees per second. Fig. 9(b) shows the rotors at 0 degrees. Fig. 9(c) shows the rotors at 90 degrees. The plane’s actual weight is 8.1 pounds. The plane's center of gravity is situated at 25% of its chord length.

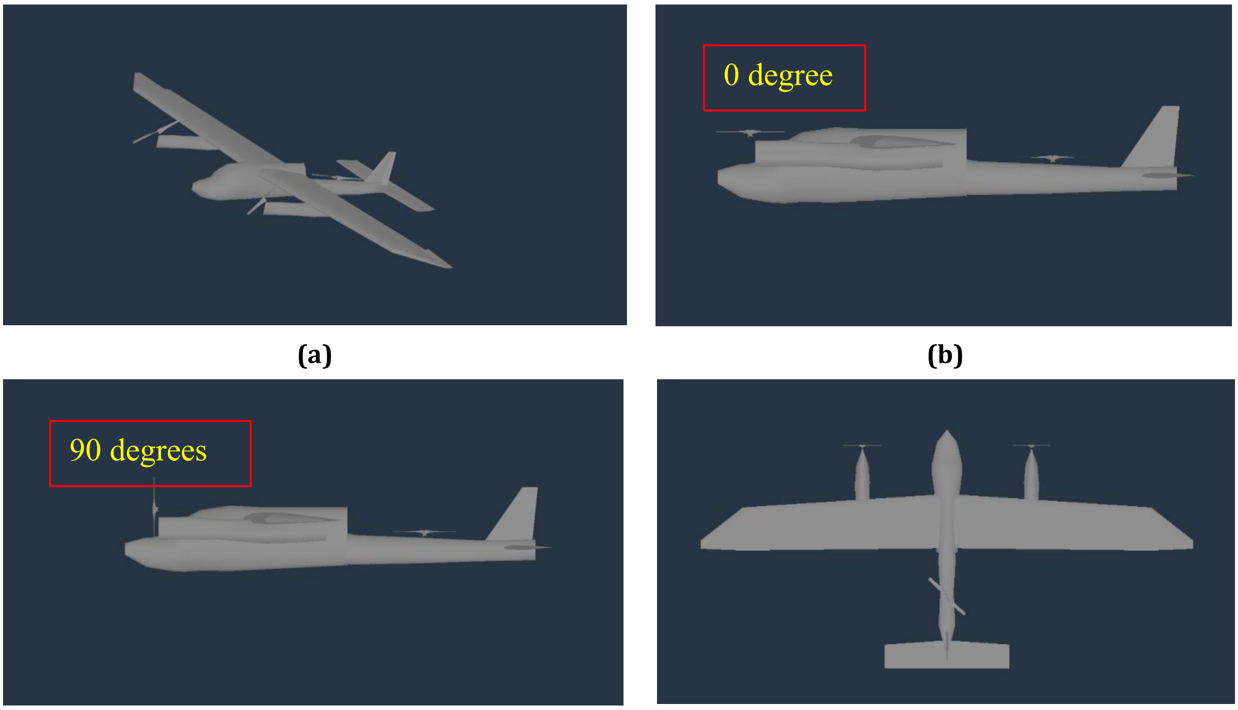

(a) **(b)**

(c) **(d)**

Fig. 9 *(a) Isometric view of tricopter UAV in Plane-maker; (b) Rotors at 0 degree; (c) Rotors at 90 degrees; (d) Top view of tricopter UAV*

Flight experiments have been conducted in the simulation to assess the tricopter's performance from transition mode to cruising mode in order to validate the design. The flight was initiated at a 10 nm approach to conduct the test. The ideal weather conditions are established for the simulation.

3. Results and Discussion

The simulation of the hover-to-forward flight transition phase was done using X-Plane by using a 10 nm approach to flying the plane. The simulation started with a hover at 4000 feet with no weather effects. The simulation took around 18 seconds. The transition from hover to forward flight occurs between the 5th and 10th seconds.

3.1 Static Pitch Stability Analysis

The simulation was conducted to evaluate the pitch stability parameters of a VTOL Tricopter UAV during the hover-to-forward transition phase. Table 2 shows the value of C_m (pitching moment coefficient) and Alpha (angle of attack) for analyzing pitch stability. The static pitch stability data indicates, as shown in Fig. 10, a typical behavior for a VTOL UAV transitioning from hover to forward flight. Initially, during the hovering phase from 1st to 3rd seconds, the tricopter shows stable hovering in hover mode, with C_m values ranging from -2.0314 to -5.7387 and alpha values ranging from 1.9553 to 1.9749 degrees. A rise in Alpha values leads to a negative pitching moment. The slope of the C_m vs. Alpha curve is negative, as shown in Fig. 10, indicating stability during hover [12].

Table 2 *C_m vs Alpha*

Time (sec)	C_m	Alpha (degree)	Rotor tilt (degree)	Phase
1	-2.0314	1.9553	0	Hovering phase
2	-2.1159	1.9619	0	
3	-5.6103	1.9749	0	
4	1.6052	2.2166	Transition starts	
5	2.0048	2.3379	15	During transition
6	1.7822	2.5481	30	
7	0.8372	2.9908	45	
8	0.2927	3.6607	60	
9	0.1654	4.1815	75	
10	-0.0713	5.2412	90	
11	-0.3776	6.1672	90	Forward phase
12	-0.4939	4.3879	90	
13	-0.4331	2.1888	90	
14	0.9402	3.2841	90	
15	0.8175	3.5601	90	
16	0.7515	3.9801	90	
17	0.137	4.6583	90	
18	-0.1858	5.2653	90	

The transition starts at the 4th second, the C_m value rises to 1.6052, and the angle of attack is 2.2166°, which represents instability in this region. During the transition phase from 5th to 10th seconds, as shown in Fig. 11, the C_m again rises to 2.0048 and alpha also rises to 2.3379° showing a continued nose-up moment, which also represents instability at 5th second. However, as the phase progresses, C_m values decrease and eventually become negative -0.0713 as alpha increases from 2.3379° to 5.2412°. This trend indicates the tricopter UAV adjusts towards stability by developing a nose-down moment as alpha increases.

The graph in Fig. 12 shows that the C_m values oscillate between positive and negative during the forward flight phase from 11 to 18 seconds, indicating dynamic adjustments in response to fluctuating Alpha values. This phase demonstrates that the tricopter UAV consistently modifies its pitch to maintain stability. Negative C_m values (-0.3776 to -0.4939) at higher Alpha angles (6.1672° to 4.3879°) signify a stable nose-down moment. Conversely, at 13 to 14 seconds, there is a minor increase in C_m values from -0.4331 to 0.9402, indicating a phase of slight instability in the tricopter UAV during forward motion. Subsequently, C_m levels began to decrease as alpha values increased, thus indicating stability.

During the hovering phase, the tricopter UAV is stable with negative C_m values, maintaining a nose-down moment with positive alpha (AOA) values. At the beginning of the transition phase, there is potential instability with the increase of C_m values as alpha values increase. Stability improves as C_m values decrease and eventually become negative, indicating the UAV adjusts to a stable forward flight. After the transition phase, the tricopter UAV exhibits stability with fluctuations in Cm and Alpha. The presence of both positive and negative C_m values indicates ongoing adjustments to maintain stable forward flight. But at some instant, it shows a slight instability. An aircraft can be considered to have static pitch stability if the slope of the C_m vs. Alpha curve is negative. A rise in Alpha (angle of attack) leads to a negative (nose-down) pitching moment. This causes the nose to move downward and decreases the angle of attack, thus returning the aircraft to its original position [12].

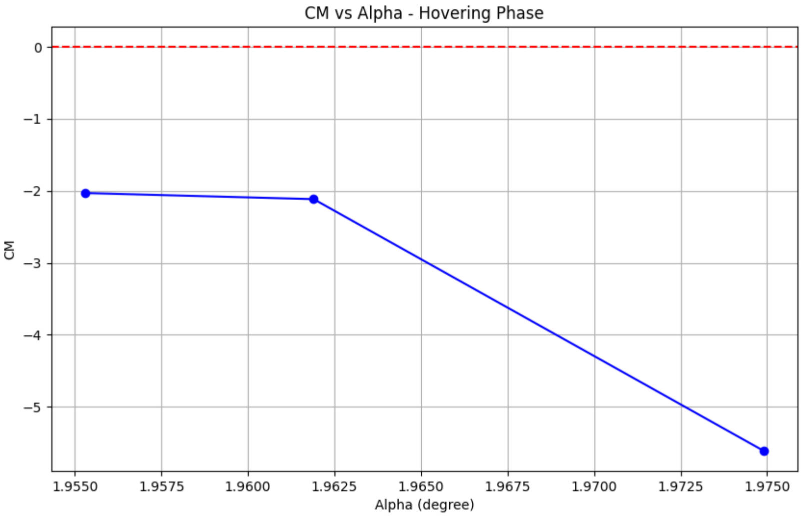

Fig. 10 *C_m vs Alpha (degree) during hovering phase*

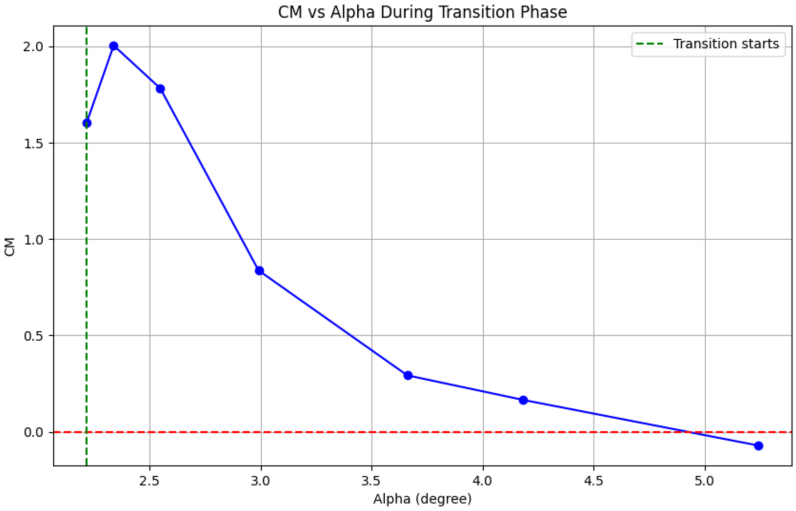

Fig. 11 *C_m vs Alpha (degree) during transition phase*

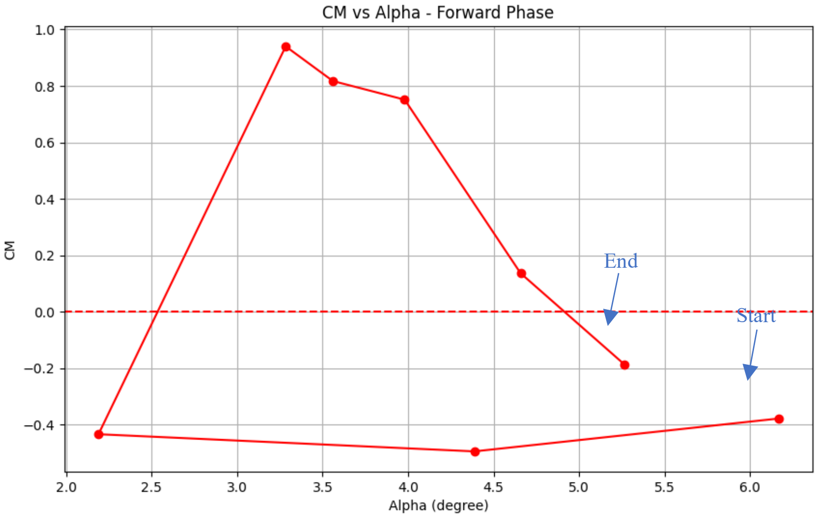

Fig. 12 *C_m vs Alpha (degree) during forward phase*

3.2 Thrust Analysis

The data derived from the simulation, illustrated in Table 3, provides significant insights into the performance of the VFW tricopter UAV during the hover-forward transition phase. Figure 13 illustrates that at the commencement of the simulation, the VFW tricopter UAV generated a thrust of 10.62 lbf, enabling the necessary vertical lift for takeoff. During the interval of 1 to 3 seconds in the hovering phase, the thrust remains very stable at around 10.62–10.79 lbf. The tricopter's capacity to sustain a hovering position prior to commencing the transition demonstrates its stability. At 4 seconds, the thrust attained 10.863 lbf, signifying the starting phase of the transition flight. Throughout the interval from 5 to 10 seconds, the thrust progressively decreases from 9.85 lbf to a minimum of 2.6 lbf at the 10-second mark. This signifies a transition from hover mode to forward mode. Upon completion of the transition phase, the tricopter's thrust stabilizes, signifying a successful shift to forward flight. From 11 to 18 seconds, the tricopter's thrust consistently measures around 2 to 2.3 lbf. The low thrust readings signify that the tricopter has successfully entered forward flight and is maintaining stable forward thrust. Research findings demonstrate a consistent variation in thrust during the transition from hovering to forward mode. The tricopter first produces significant push to achieve hover, which gradually diminishes as it transitions to forward motion, ultimately stabilizing at reduced levels to maintain that motion [13].

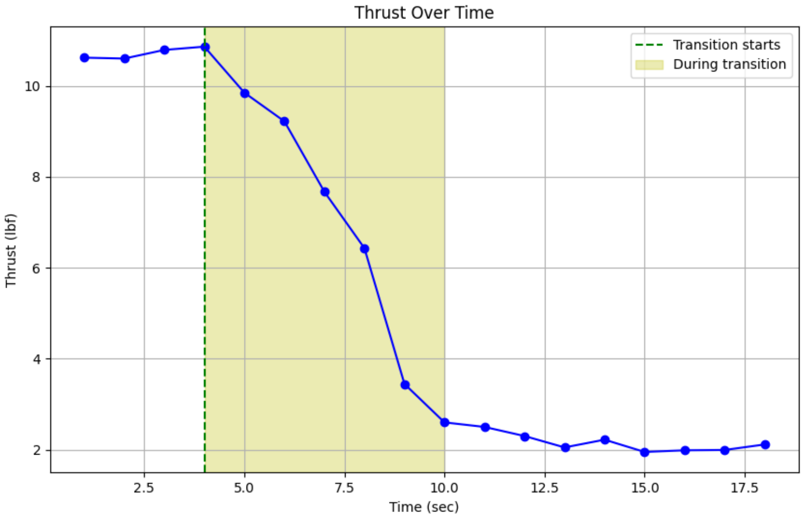

Fig. 13 *Thrust over time*

Table 3 *Thrust over time*

Time (sec)	Thrust (Ibf)	Rotor tilt (degree)	Phase
1	10.62	0	Hovering phase
2	10.6	0	
3	10.79	0	
4	10.862	Transition starts	
5	9.85	15	During transition
6	9.22	30	
7	7.67	45	
8	6.43	60	
9	3.445	75	
10	2.6	90	
11	2.5	90	Forward phase
12	2.3	90	
13	2.05	90	
14	2.22	90	
15	1.9502	90	
16	1.9864	90	
17	1.9941	90	
18	2.115	90	

3.3 Lift and Drag forces

The data obtained from the simulation, as shown in Table 4, provides insights into the lift and drag forces acting on the VTOL tricopter during the hover-forward transition phase. The dynamic action of air generates lift force by creating pressure differences on various parts of the aircraft, primarily the wings. It works perpendicular to the direction of flight and the aircraft's lateral axis through the center of pressure. In level flight, the lift force counteracts the downward force of weight [14].

Figure 14 shows the lift forces produced by the tricopter during all flight phases. During the hovering phase, which lasted 1-3 seconds, the rotors generated the necessary vertical lift for takeoff, as evidenced by the first recorded lift force of 9.05 lbf. The lift force consistently measures roughly 9.05 to 9.705 lbf. This illustrates the tricopter's ability to maintain a hover. At 4 seconds into the transition, there is a noticeable reduction in lift force, which decreases to 9.462 lbf, signifying a decline in vertical lift as forward motion initiates. In the transition phase, the lift force progressively decreases, ultimately reaching a value of 6.465 lbf at 10 seconds. This reduction is expected as the tricopter UAV transitions from hover to forward mode. Following the transition phase from 11 to 18 seconds, the lift force significantly decreases, attaining 5.488 lb at 11 seconds and subsequently declining to 3.499 lbf at 12 seconds. This indicates that the rotors promptly diminished their thrust following the shift. Subsequently, the lift force undergoes a progressive increase from 8.8 to 10.13 lbf between 13 and 14 seconds. The lift attains a consistent range of 7.185 to 6.414 lbf by the conclusion of the forward phase. The variations suggest that the VTOL tricopter UAV achieves vertical lift via its wings during forward flight mode.

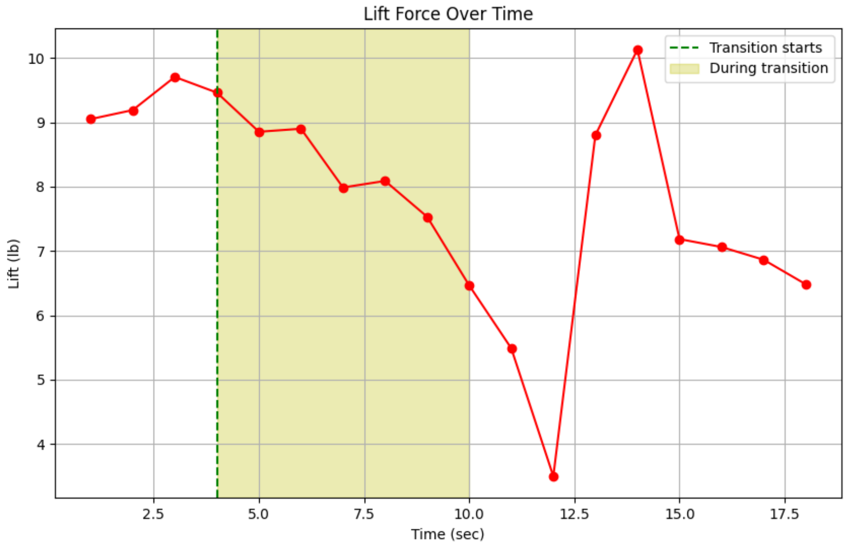

Fig. 14 *Lift force over time*

The wing, rotor, fuselage, and other projecting elements produce drag, a force that obstructs airflow and acts as a retarding force against the aircraft's motion. The drag force is a resistance that opposes the relative wind's direction. [14]. Figure 15 illustrates the drag forces exerted on airplanes throughout all phases of flight. The hovering phase occurs from 1 to 3 seconds, exhibiting a considerable drag force of approximately 1.056 to 1.077 lbf. This signifies that the UAV experienced a certain degree of drag force while hovering. Minor adjustments in hovering stability can also account for the variations in drag force. At 4 seconds, as the transition commences, the drag force begins to diminish. This was expected when the tricopter UAV's rotors began to tilt forward to initiate its forward drive. During the interval from 5 to 10 seconds, the drag force steadily decreases, ultimately reaching a value of 0.387 lbf at the 10-second mark. The decrease in drag occurs due to the reduction in the frontal area of the tricopter UAV. In the forward phase, spanning from 11 to 18 seconds, the drag force diminishes from 0.337 lbf at 11 seconds to a minimum of 0.243 lbf at 12 seconds. Upon reaching the minimum, the drag force subsequently increases, peaking at 0.641 lbf. After 14 seconds, it stabilizes at around 0.5 lbf toward the end of the forward phase. The fluctuations in these values signify that the UAV adjusts its velocity and orientation during forward motion.

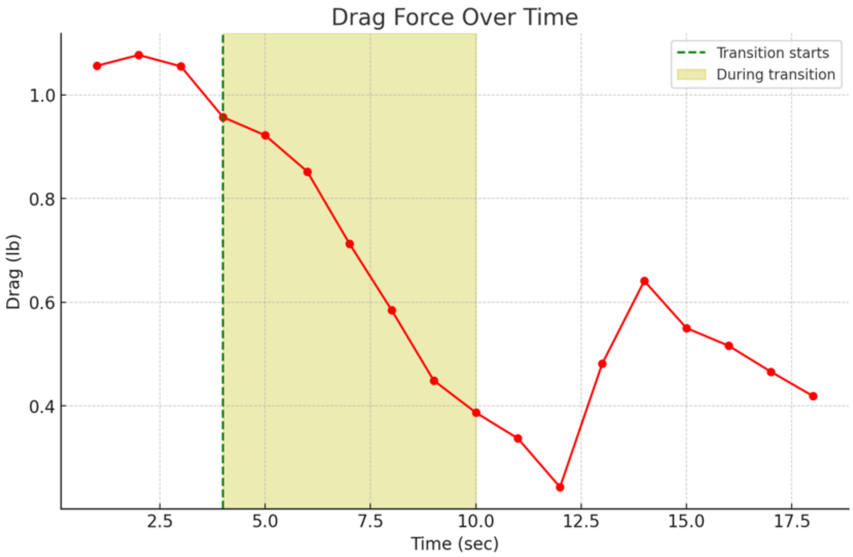

Fig. 15 *Drag force over time*

Table 4 *Lift and Drag forces over time*

Time (sec)	Lift (lbf)	Drag (Ibf)	Rotor tilt (degree)	Phase
1	9.05	1.056	0	Hovering phase
2	9.19	1.077	0	
3	9.705	1.055	0	
4	9.462	0.957	Transition starts	
5	8.853	0.922	15	During transition
6	8.9	0.852	30	
7	7.987	0.713	45	
8	8.089	0.585	60	
9	7.532	0.449	75	
10	6.465	0.387	90	
11	5.488	0.337	90	Forward phase
12	3.499	0.243	90	
13	8.8	0.481	90	
14	10.13	0.641	90	
15	7.185	0.55	90	
16	7.062	0.516	90	
17	6.864	0.466	90	
18	6.484	0.419	90	

4. Conclusion

The objectives of this project, which are to design VFW tricopter UAV using Plane-maker and conduct simulations in X-Plane to analyze the aerodynamic characteristics of the plane during the hover-to-forward transition phase have been successfully achieved. The simulation revealed key insights into the UAV's static pitch stability, thrust, lift, and drag forces. In terms of static pitch stability, initially, the VFW tricopter UAV consistently produces negative C_m during hovering, which causes it to have a nose-down tendency. However, as indicated by the negative slope of C_m vs. Alpha, the UAV is statically stable. Then, at the beginning of the transition phase, there is potential instability with the increase of C_m values as alpha values increase. But afterwards, it becomes stable as C_m values decrease and eventually become negative, indicating the UAV adjusts to a stable forward flight. The instability at the beginning of the transition phase might be due to the changing of the thrust vector during the transition.

It has been found that the value of thrust force is considerably good for vertical takeoff and forward flights. Before the transition, the thrust was high for vertical lift and maneuvering, but after the transition, the thrust went down to make the plane glide. Lift force was high and stable during hover, decreased during transition, and showed fluctuations as the tricopter UAV adjusted to forward flight. Drag force was relatively high during hover and decreased during transition, stabilizing at lower values during forward flight, indicating successful aerodynamic adjustment. Overall, simulation data is crucial for optimizing the VTOL tricopter's design and enhancing its flight performance, contributing to the advancement of UAV technology in diverse applications. This project helps to cover the knowledge gap in understanding the VFW tricopter UAV's behavior during transition.

Acknowledgement

The authors are grateful for the financial support received from the Ministry of Higher Education under the Fundamental Research Grant Scheme (FRGS), Code K330, as well as the Faculty of Mechanical and Manufacturing Engineering at Universiti Tun Hussein Onn Malaysia.

Conflict of Interest

Authors declare that there is no conflict of interest regarding the publication of the paper.

Author Contribution

The authors confirm their contribution to the paper as follows. ***Study conception and design:*** *Muhammad Munib Abid Aqeel, Mohd Fadhli Zulkafli and Mohammad Fahmi Pairan;* ***Data collection:*** *Muhammad Munib Abid Aqeel and Mohammad Fahmi Pairan;* ***Analysis and interpretation of results:*** *Muhammad Munib Abid Aqeel and Mohd Fadhli Zulkafli;* ***Draft manuscript preparation:*** *Muhammad Munib Abid Aqeel and Mohd Fadhli Zulkafli. All authors reviewed the results and approved the final version of the manuscript.*

References

[1] M. Hassanalian, A. Abdelkefi, Classifications, applications, and design challenges of drones: A review, Progress in Aerospace Sciences, Volume 91, 2017, pages 99-131, ISSN 0376-0421, https://doi.org/10.1016/j.paerosci.2017.04.003.

[2] Yuksek, B., Vuruskan, A., Ozdemir, U. et al. Transition Flight Modeling of a Fixed-Wing VTOL UAV. J Intell Robot Syst 84, 83–105 (2016). https://doi.org/10.1007/s10846-015-0325-9.

[3] Tielin, M.; Chuanguang, Y.; Wenbiao, G.; Zihan, X.; Qinling, Z.; Xiaoou, Z. Analysis of technical characteristics of fixed-wing VTOL UAV. Proceedings of the IEEE International Conference on Unmanned Systems (ICUS); Beijing, China, 27–29 October 2017; pp. 293-297.

[4] Nugroho, G.; Zuliardiansyah, G.; Rasyiddin, A.A. Performance Analysis of Empennage Configurations on a Surveillance and Monitoring Mission of a VTOL-Plane UAV Using a Computational Fluid Dynamics Simulation. Aerospace; 2022; 9, 208. [DOI: https://dx.doi.org/10.3390/aerospace9040208].

[5] Zaludin, Z.; Gires, E. Automatic Flight Control Requirements for Transition Flight Phases When Converting Long Endurance Fixed Wing UAV to VTOL Aircraft. In Proceedings of the 2019 IEEE International Conference on Automatic Control and Intelligent Systems (I2CACIS), Selangor, Malaysia, 29 June 2019; pp. 273–278

[6] Martins, L.S.N. Development of a Flight Simulation Training Device and Remote Pilot Station: The URBLOG Unmanned Hybrid Airship Vehicle Case; Universidade Beira Interior: Covilhã, Portugal, 2020

[7] Li Yu, Guang He, Shulong Zhao, Xiangke Wang, Lincheng Shen, “Design and Implementation of a Hardware-in-the-Loop Simulation System for a Tilt Trirotor UAV", Journal of Advanced Transportation, Journal of Advanced Transportation, vol. 2020, Article ID 4305742, 17 pages, 2020.

[8] A. Bittar, H. V. Figueiredo, P. A. Guimaraes, and A. C. Mendes, “Guidance software-in-the-loop simulation using X-Plane and simulink for uavs,” in Proceedings of the 2014 International Conference on Unmanned Aircraft Systems (ICUAS), pp. 993–1002, IEEE, Orlando, FL, USA, May 2014.

[9] A. Bittar, N. M. F. De Oliveira, and H. V. De Figueiredo, "Hardware-in-the-loop simulation with X-plane of attitude control of a SUAV exploring atmospheric conditions, " J. Intell. Robot. Syst. Theory Appl., vol. 73, no. 1-4, pp. 271-287, 2014.

[10] C. W. Thong, Modeling Aircraft Performance and Stability on X-Plane, Australian Defence Force Academy, Canberra, Australia, 2010.

[11] Kamrani, Farzad & Ayani, Rassul. (2007). Using On-line Simulation for Adaptive Path Planning of UAVs. 167-174. 10.1109/DS-RT.2007.45.

[12] Michael V. Cook, Chapter 9 - Stability, Editor(s): Michael V. Cook, Flight Dynamics Principles (Third Edition), Butterworth-Heinemann, 2013, Pages 243-258, ISBN 9780080982427, https://doi.org/10.1016/B978-0-08-098242-7.00009-2.

[13] B. Theys, G. De Vos and J. De Schutter, "A control approach for transitioning VTOL UAVs with continuously varying transition angle and controlled by differential thrust," *2016 International Conference on Unmanned Aircraft Systems (ICUAS)*, Arlington, VA, USA, 2016, pp. 118-125, doi: 10.1109/ICUAS.2016.7502519.

[14] Harun, Mohamad Haniff & Abdullah, S. & Mohd Aras, Mohd Shahrieel & Bahar, Mohd & Ali, Fariz. (2023). “3D collision avoidance system for unmanned aerial vehicle (UAV) with decentralized approach,” IIUM Engineering Journal. 24. 373-390. 10.31436/iiumej.v24i2.2803.